



Deposited via The University of Leeds.

White Rose Research Online URL for this paper:

<https://eprints.whiterose.ac.uk/id/eprint/141066/>

Version: Accepted Version

Article:

Huntul, MJ and Lesnic, D (2019) Time-Dependent Reaction Coefficient Identification Problems with a Free Boundary. *International Journal for Computational Methods in Engineering Science & Mechanics*, 20 (2). pp. 99-114. ISSN: 1550-2287

<https://doi.org/10.1080/15502287.2019.1568619>

(c) 2019 Taylor & Francis Group, LLC. This is an Accepted Manuscript of an article published by Taylor & Francis in *International Journal for Computational Methods in Engineering Science and Mechanics* on 17 Feb 2019, available online: <https://doi.org/10.1080/15502287.2019.1568619>.

Reuse

Items deposited in White Rose Research Online are protected by copyright, with all rights reserved unless indicated otherwise. They may be downloaded and/or printed for private study, or other acts as permitted by national copyright laws. The publisher or other rights holders may allow further reproduction and re-use of the full text version. This is indicated by the licence information on the White Rose Research Online record for the item.

Takedown

If you consider content in White Rose Research Online to be in breach of UK law, please notify us by emailing eprints@whiterose.ac.uk including the URL of the record and the reason for the withdrawal request.

Time-dependent reaction coefficient identification problems with a free boundary

M.J. Huntul^{1,2} and D. Lesnic¹

¹*Department of Applied Mathematics, University of Leeds, Leeds LS2 9JT, UK*

²*Department of Mathematics, Faculty of Science, Jazan University, P.O. Box 114, Jazan 45142, Saudi Arabia*

E-mails : mmmjmh@leeds.ac.uk (M.J. Huntul), amt5ld@maths.leeds.ac.uk (D. Lesnic).

Abstract

The determination of time-dependent reaction coefficients in free boundary heat transfer problems is, for the first time, numerically investigated. The additional data which provides a unique solution is given by the Stefan boundary condition and the heat moments. The finite difference method with the Crank-Nicolson scheme combined with a regularized nonlinear optimization are employed. The resulting nonlinear system of equations is solved numerically using the MATLAB toolbox routine *lsqnonlin* for minimizing the Tikhonov regularization functional. A discussion of the choice of regularization parameters is provided. Numerical results are presented and discussed.

Keywords: Inverse problem; Free boundary; Heat equation; Tikhonov regularization.

1 Introduction

Coefficient identification problems involving an unknown free boundary are some of the most complicated and practically important problems, [18,19,21], and the Stefan problem is a particular example, [5,7].

In [2,12], the authors investigated free boundary problems with nonlinear diffusion. The numerical solution of inverse Stefan problems based on the method of fundamental solutions has been investigated in [13,14]. The determination of time-dependent thermal coefficients was solved using the method of suboptimal stage-by-stage optimization in [3]. The heat equation with an unknown time-dependent thermal diffusivity or heat source in a domain with a free boundary has been investigated in [11] and [17], respectively. Time-dependent thermal conductivity identifications subject to various kind of overdetermination conditions have been studied in [15].

In recent papers, [8–10], the authors have investigated the identification of multiple time-dependent coefficients together with an unknown free boundary. Continuing these analyses, in this paper, we investigate the numerical reconstruction of time-dependent reaction coefficients in the heat equation with a free boundary subject to initial, Dirichlet and Stefan boundary conditions, as well as heat moment measurements. It should be noted that the fundamental contribution of this work is the proposal of a regularization algorithm to solve the identification problem and its numerical realization.

The paper is structured in the following way. The mathematical formulation of the inverse problems are formulated in Section 2. The numerical solution for the direct problem based on the finite difference method (FDM) with the Crank-Nicolson scheme is briefly

mentioned in Section 3. In Section 4, the numerical approach based on the minimization of the nonlinear Tikhonov regularization functional is introduced. Numerical results are presented and discussed in Section 5. Finally, conclusions are presented in Section 6.

2 Mathematical formulation

Consider the one-dimensional time-dependent parabolic heat equation

$$\frac{\partial u}{\partial t}(x, t) = a(x, t) \frac{\partial^2 u}{\partial x^2}(x, t) + b(x, t) \frac{\partial u}{\partial x}(x, t) + (c_1(t)x + c_2(t))u(x, t) + f(x, t),$$

$$(x, t) \in \Omega_T, \quad (1)$$

for the unknown temperature $u(x, t)$ in the moving domain $\Omega_T = \{(x, t) | 0 < x < h(t), 0 < t < T\}$ with unknown free boundary $x = h(t) > 0$ and time-dependent coefficients $c_1(t)$ and $c_2(t)$, subject to the initial condition

$$u(x, 0) = \phi(x), \quad 0 \leq x \leq h(0) =: h_0, \quad (2)$$

where $h_0 > 0$ is given, the Dirichlet boundary conditions

$$u(0, t) = \mu_1(t), \quad u(h(t), t) = \mu_2(t), \quad t \in [0, T], \quad (3)$$

and the over-determination conditions

$$h'(t) + u_x(h(t), t) = \mu_3(t), \quad t \in [0, T], \quad (4)$$

$$\int_0^{h(t)} u(x, t) dx = \mu_4(t), \quad t \in [0, T], \quad (5)$$

$$\int_0^{h(t)} xu(x, t) dx = \mu_5(t), \quad t \in [0, T], \quad (6)$$

where $\phi(x)$ and $\mu_i(t)$ for $i = \overline{1, 5}$ are given functions. We assume that the functions in the above equations are sufficiently regular as required in the sequel and that the input data (2)–(6) are compatible.

Equation (4) represents a Stefan interface moving boundary condition. Also, equations (5) and (6) represent the specification of the energy (or mass) and heat momentum, respectively. In equation (1), the coefficients a and b representing diffusion and convection/advection are assumed to be known, as is the heat source f . Note that from (2) and (5) we can, in fact, obtain h_0 as a positive solution of the equation $\mu_4(0) = \int_0^{h_0} \phi(x) dx$. Finally, remark that the reaction coefficient in (1) is linearly dependent on the space variable x with two unknown time-dependent coefficients $c_1(t)$ and $c_2(t)$. This can also be seen as a particular case of a space and time-dependent blood perfusion coefficient in bio-heat transfer, [23].

First, the change of variable $y = x/h(t)$ is performed, [21], to reduce the problem (1)–(6) to the following inverse problem for the unknowns $h(t)$, $c_1(t)$, $c_2(t)$ and $v(y, t) := u(yh(t), t)$:

$$\frac{\partial v}{\partial t}(y, t) = \frac{a(yh(t), t)}{h^2(t)} \frac{\partial^2 v}{\partial y^2}(y, t) + \frac{b(yh(t), t) + yh'(t)}{h(t)} \frac{\partial v}{\partial y}(y, t)$$

$$+ (yh(t)c_1(t) + c_2(t))v(y, t) + f(yh(t), t), \quad (y, t) \in Q_T, \quad (7)$$

in the fixed domain $Q_T := \{(x, t) | 0 < y < 1, 0 < t < T\} = (0, 1) \times (0, T)$,

$$v(y, 0) = \phi(yh_0), \quad y \in [0, 1], \quad (8)$$

$$v(0, t) = \mu_1(t), \quad v(1, t) = \mu_2(t), \quad t \in [0, T], \quad (9)$$

$$h'(t) + \frac{1}{h(t)}v_y(1, t) = \mu_3(t), \quad t \in [0, T], \quad (10)$$

$$h(t) \int_0^1 v(y, t) dy = \mu_4(t), \quad t \in [0, T], \quad (11)$$

$$h^2(t) \int_0^1 yv(y, t) dy = \mu_5(t), \quad t \in [0, T]. \quad (12)$$

The uniqueness of a solution of the inverse problem (7)–(12) has been established in [21] and reads as follows.

Theorem 1. *Assume that*

$a \in C^{2,0}([0, \infty) \times [0, T])$, $b, f \in C^{1,0}([0, \infty) \times [0, T])$, $a(x, t) > 0$, $(x, t) \in [0, \infty) \times [0, T]$,

$$\phi(x) \geq \phi_0 > 0, \quad x \in [0, \infty), \quad \mu_i(t) > 0, \quad i = 1, 2, 4, \quad t \in [0, T].$$

Then, a solution $(h, c_1, c_2, v) \in C^1[0, T] \times (C[0, T])^2 \times C^{2,1}(\overline{Q_T})$, $h(t) > 0, t \in [0, T]$, of the problem (7)–(12) is unique.

Remark 1.

(i) We remark that the values of $c_1(0)$ and $c_2(0)$ can be determined using the compatibility of input data in (1)–(6). Indeed, first observe that by differentiating (5) and (6) with respect to t and integrating (1) with respect to x we obtain

$$\begin{aligned} \mu_4'(t) - h'(t)\mu_2(t) &= \int_0^{h(t)} u_t(x, t) dx = \int_0^{h(t)} \left(a(x, t)u_{xx}(x, t) + b(x, t)u_x(x, t) \right) dx \\ &\quad + c_1(t)\mu_5'(t) + c_2(t)\mu_4'(t) + \int_0^{h(t)} f(x, t) dx, \quad t \in [0, T], \end{aligned} \quad (13)$$

$$\begin{aligned} \mu_5'(t) - h(t)h'(t)\mu_2(t) &= \int_0^{h(t)} xu_t(x, t) dx = \int_0^{h(t)} x \left(a(x, t)u_{xx}(x, t) + b(x, t)u_x(x, t) \right) dx \\ &\quad + c_1(t) \int_0^{h(t)} x^2u(x, t) dx + c_2(t)\mu_5'(t) + \int_0^{h(t)} xf(x, t) dx, \quad t \in [0, T]. \end{aligned} \quad (14)$$

Also, (4) yields

$$h'(t) = \mu_3(t) - u_x(h(t), t), \quad t \in [0, T]. \quad (15)$$

Applying the compatibility of the data (2)–(6) at $t = 0$ in (13)–(15) imposed at $t = 0$ results in:

$$\begin{cases} c_1(0)\mu_5(0) + c_2(0)\mu_4(0) = \mu_4'(0) - \mu_2(0)\left(\mu_3(0) - \phi'(h_0)\right) - \int_0^{h_0} f(x, 0)dx \\ - \int_0^{h_0} \left(a(x, 0)\phi''(x) + b(x, 0)\phi'(x)\right)dx, \\ c_1(0)\int_0^{h_0} x^2\phi(x)dx + c_2(0)\mu_5(0) = \mu_5'(0) - h_0\mu_2(0)\left(\mu_3(0) - \phi'(h_0)\right) - \int_0^{h_0} xf(x, 0)dx \\ - \int_0^{h_0} x\left(a(x, 0)\phi''(x) + b(x, 0)\phi'(x)\right)dx. \end{cases} \quad (16)$$

This system of two linear equations with two unknowns has a unique solution determined by the data (2)–(6) at $t = 0$ if and only if the determinant of the system is non-zero, i.e.

$$\mu_5^2(0) - \mu_4(0)\int_0^{h_0} x^2\phi(x)dx \neq 0.$$

From (5), (6) and using that $\phi > 0$ and Cauchy's inequality we immediately obtain that

$$\mu_5^2(0) - \mu_4(0)\int_0^{h_0} x^2\phi(x)dx = \left(\int_0^{h_0} x\phi(x)dx\right)^2 - \left(\int_0^{h_0} \phi(x)dx\right)\left(\int_0^{h_0} x^2\phi(x)dx\right) < 0,$$

and therefore the system of equations (16) has a unique solution indeed.

(ii) As remarked in [8, 10, 18], the Stefan condition (4) can be replaced by the second-order moment specification

$$\int_0^{h(t)} x^2u(x, t)dx = \mu_6(t), \quad t \in [0, T], \quad (17)$$

or, in terms of the variable v , by

$$h^3(t)\int_0^1 y^2v(y, t)dy = \mu_6(t), \quad t \in [0, T]. \quad (18)$$

(iii) Sufficient conditions for the local existence of solution of the inverse problems were also provided in [18, 21].

3 Solution of direct problem

In this section we consider the direct initial boundary value problem given by equations (7)–(9), where $h(t)$, $c_1(t)$, $c_2(t)$, $a(x, t)$, $b(x, t)$, $f(x, t)$, $\phi(x)$, and $\mu_i(t)$, $i = 1, 2$, are known and the solution $v(y, t)$ is to be determined together with the quantities of interest $\mu_i(t)$, $i = \overline{3, 6}$. To achieve this, we use the FDM with the Crank-Nicolson scheme, [10], based on subdividing the solution domain $Q_T = (0, 1) \times (0, T)$ into M and N subintervals of equal step lengths Δy and Δt , where $\Delta y = 1/M$ and $\Delta t = T/N$, respectively. This implicit scheme is unconditionally stable and is second-order accurate in space and first-order accurate in time. At the node (i, j) we denote $v(y_i, t_j) = v_{i,j}$, where $y_i = i\Delta y$, $t_j = j\Delta t$, $a(y_i, t_j) = \overline{a_{i,j}}$, $b(y_i, t_j) = \overline{b_{i,j}}$, $h(t_j) = h_j$, $c_1(t_j) = \overline{c1_j}$, $c_2(t_j) = \overline{c2_j}$, and $f(y_i, t_j) = \overline{f_{i,j}}$ for $i = \overline{0, M}$ and $j = \overline{0, N}$. The expressions in equations (10)–(12) and (18) are calculated using the following finite difference approximation formula and trapezoidal rule for integrals:

$$\mu_3(t_j) = \frac{h_j - h_{j-1}}{\Delta t} - \frac{4v_{M-1,j} - v_{M-2,j} - 3v_{M,j}}{2(\Delta y)h_j}, \quad j = \overline{1, N}, \quad (19)$$

$$\mu_{k+3}(t_j) = \frac{h_j^k}{2N} \left(y_0^{k-1} v_{0,j} + y_M^{k-1} v_{M,j} + 2 \sum_{i=1}^{M-1} y_i^{k-1} v_{i,j} \right), \quad j = \overline{1, N}, \quad k = 1, 2, 3. \quad (20)$$

4 Numerical approach to solve the inverse problem

In this section, we wish to obtain a simultaneous stable determination of the two unknown coefficients $c_1(t)$ and $c_2(t)$, together with the free boundary $h(t)$ and the transformed temperature $v(y, t)$, satisfying equations (7)–(12), or (7)–(9), (11), (12) and (18). Nevertheless, since the inverse problems under investigation are ill-posed there is scope to regularize and then discretize, but due to the nonlinearity of the coefficient identification problems and because the minimization is performed numerically using an exterior toolbox routine, we proceed the other way around by first discretizing and afterwards regularizing. Therefore, we formulate the inverse problems as a nonlinear minimization of the Tikhonov regularization function

$$\begin{aligned} F(\mathbf{h}, \mathbf{c}_1, \mathbf{c}_2) = & \sum_{j=1}^N \left[\frac{h_j - h_{j-1}}{\Delta t} + \frac{v_y(1, t_j)}{h_j} - \mu_3(t_j) \right]^2 + \sum_{j=1}^N \left[h_j \int_0^1 v(y, t_j) dy - \mu_4(t_j) \right]^2 \\ & + \sum_{j=1}^N \left[h_j^2 \int_0^1 y v(y, t_j) dy - \mu_5(t_j) \right]^2 + \beta_1 \sum_{j=1}^N (h_j - h_j^*)^2 + \beta_2 \sum_{j=1}^N (c_{1j} - c_{1j}^*)^2 \\ & + \beta_3 \sum_{j=1}^N (c_{2j} - c_{2j}^*)^2, \quad (21) \end{aligned}$$

or,

$$\begin{aligned} F(\mathbf{h}, \mathbf{c}_1, \mathbf{c}_2) = & \sum_{j=1}^N \left[h_j \int_0^1 v(y, t_j) dy - \mu_4(t_j) \right]^2 + \sum_{j=1}^N \left[h_j^2 \int_0^1 y v(y, t_j) dy - \mu_5(t_j) \right]^2 \\ & + \sum_{j=1}^N \left[h_j^3 \int_0^1 y^2 v(y, t_j) dy - \mu_6(t_j) \right]^2 + \beta_1 \sum_{j=1}^N (h_j - h_j^*)^2 + \beta_2 \sum_{j=1}^N (c_{1j} - c_{1j}^*)^2 \\ & + \beta_3 \sum_{j=1}^N (c_{2j} - c_{2j}^*)^2, \quad (22) \end{aligned}$$

where v solves (7)–(9) for given (h, c_1, c_2) , that is, at each iteration n , the FDM of Section 3 is employed to solve the direct problem (7)–(9) with given coefficients h^n , c_1^n and c_2^n . In (21) and (22), \mathbf{h}^* , \mathbf{c}_1^* and \mathbf{c}_2^* represent some *a priori* estimates of the solution of the inverse problem that are of great importance to be able to apply the scheme of regularization of Tikhonov, ([6], Chapter 10).

The minimization of the objective function (21), or (22), is performed using the MATLAB toolbox routine *lsqnonlin*, which does not require supplying by the user the gradient of the objective function, [16]. This routine attempts to find the minimum of a sum of squares by starting from the initial guesses \mathbf{h}^0 , \mathbf{c}_1^0 and \mathbf{c}_2^0 for \mathbf{h} , \mathbf{c}_1 and \mathbf{c}_2 , respectively, and marching to the next iterate according to a trust region reflective search method [4]. In general, it is sensible to take the *a priori* estimates \mathbf{h}^* , \mathbf{c}_1^* and \mathbf{c}_2^* be equal with the initial guesses \mathbf{h}^0 , \mathbf{c}_1^0 and \mathbf{c}_2^0 , however, in this study we take them to be zero in order to investigate a more severe search for the minimum of the nonlinear functionals (21)

and (22). Since the inverse problems under investigation have unique solutions, in case of exact data, a robust numerical search algorithm should converge to the unique solution, independent of the initial guess, i.e. it should be globally convergent. In particular, changing the penalised least-squares functionals (21) and (22) into strongly convex Carleman choices [1] will be the subject of future work.

We have compiled the routine *lsqnonlin* with the following specifications:

- Algorithm is the Trust Region Reflective (TRR) minimization, [4].
- Maximum number of iterations, (MaxIter)= $10 \times (\text{number of variables})$.
- Maximum number of objective function evaluations, (MaxFunEvals)= $10^5 \times (\text{number of variables})$.
- Termination tolerance on the function value, (TolFun) = 10^{-20} .
- Solution tolerance value, (xTol)= 10^{-20} .
- The lower and upper simple bounds are 10^{-10} and 10^3 for h , and -10^3 and 10^3 for c_1 and c_2 .

The inverse problems are solved subject to both exact and noisy input data which is numerically simulated as follows:

$$\mu_{k+2}^{\epsilon k}(t_j) = \mu_{k+2}(t_j) + \epsilon k_j, \quad j = \overline{1, N}, \quad k = \overline{1, 4}, \quad (23)$$

where ϵk_j are random variables generated from a Gaussian normal distribution with mean zero and standard deviation σ_k given by

$$\sigma_k = p \times \max_{t \in [0, T]} |\mu_{k+2}(t)|, \quad k = \overline{1, 4}, \quad (24)$$

where p represents the percentage of noise. We use the MATLAB function *normrnd*(0, σ_k , N) to generate the random variables $(\epsilon k_j)_{j=\overline{1, N}}$ for $k = \overline{1, 4}$.

5 Numerical results and discussion

In this section we investigate a couple of examples in order to assess the accuracy and stability of the numerical methods introduced in Section 3 for the direct problem based on the FDM with $M = N = 40$, and in Section 4 for the numerical approach to solve the inverse problem based on minimizing the nonlinear Tikhonov regularization objective functional (21) or (22). Furthermore, we add noise to the input data in equations (10)–(12) and (18) to mimic the real situation of measurement errors, by using equations (23) and (24). We compute the root mean squares error given by

$$rmse(h) = \left[\frac{T}{N} \sum_{j=1}^N \left(h^{numerical}(t_j) - h^{exact}(t_j) \right)^2 \right]^{1/2}, \quad (25)$$

and similar expressions exist for $c_1(t)$ and $c_2(t)$. For simplicity, we take $T = 1$ in all examples.

5.1 Example 1

We consider the inverse problem (1)–(6) with unknown coefficients $h(t)$, $c_1(t)$ and $c_2(t)$, and the input data given by

$$\begin{aligned} a(x, t) &= \frac{1}{2}(1+t) + x, & b(x, t) &= -1 - x - t, & \phi(x) &= 2 + x, & \mu_1(t) &= e^t(2+t), \\ f(x, t) &= e^t(2+t+x)(3+t+x+tx), & \mu_2(t) &= e^t(3+2t), & \mu_3(t) &= 1 + e^t, \\ \mu_4(t) &= \frac{1}{2}e^t(1+t)(5+3t), & \mu_5(t) &= \frac{1}{4}(1+t)^2(3+6t+t^2), & h_0 &= 1. \end{aligned} \quad (26)$$

One can observe that the conditions of Theorem 1 are satisfied and hence, the uniqueness of solution is guaranteed. The analytical solution is given by

$$h(t) = 1 + t, \quad c_1(t) = -1 - t, \quad c_2(t) = -1 - t, \quad (27)$$

$$u(x, t) = e^t(2 + t + x). \quad (28)$$

Also, the analytical solution for the transformed temperature $v(y, t)$ satisfying (7)–(12) is given by

$$v(y, t) = e^t(2 + t + y(1 + t)). \quad (29)$$

The initial guesses for the vectors \mathbf{h} , \mathbf{c}_1 and \mathbf{c}_2 are taken as

$$h^0(t_j) = h(0) = h_0 = 1, \quad c_1^0(t_j) = c_1(0) = -1, \quad c_2^0(t_j) = c_2(0) = -1, \quad j = \overline{1, N}, \quad (30)$$

where the values of $c_1(0)$ and $c_2(0)$ have been obtained exactly by solving the system of equations (16).

We consider first the case when there is no noise in the input data μ_3, μ_4 and μ_5 , i.e. $p = 0$ in (24). The objective function (21), as a function of a number of iterations, is plotted in Figure 1, with and without regularization. From this figure, it can be seen that a rapid monotonic decreasing convergence is achieved in a few iterations.

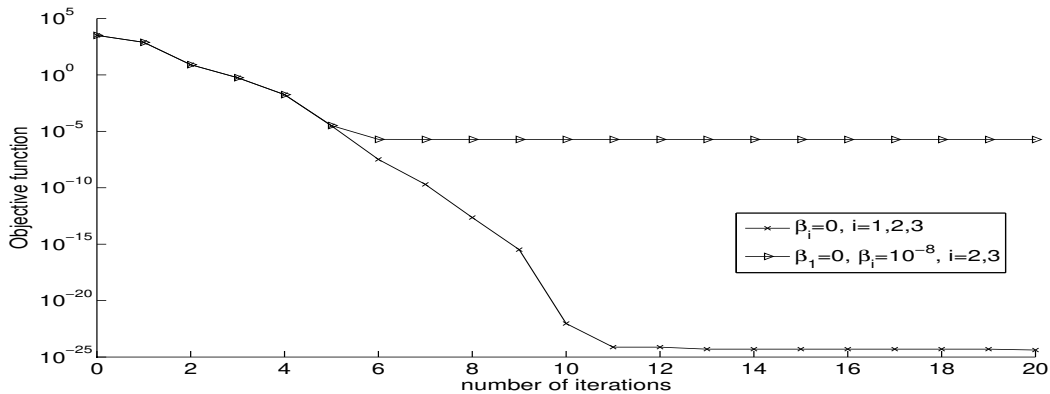


Figure 1: The objective function (21), as a function of a number of iterations, no noise, with and without regularization, for Example 1.

The *rmse* values for the unknowns coefficients $h(t)$, $c_1(t)$ and $c_2(t)$, obtained with and without regularization are presented, versus the number of iterations, in Figure 2. The corresponding numerical solutions obtained after 20 iterations (in 38 minutes computational time) are illustrated in Figure 3 (for $h(t)$, $c_1(t)$ and $c_2(t)$) and Figure 4 (for $v(y, t)$).

First, from Figure 2 it can be observed that $rmse(h)$ values are much lower than the $rmse(c_i)$, $i = 1, 2$, indicating that the free boundary $h(t)$ is retrieved more accurately than the coefficients c_1 and c_2 . Second, from Figure 2 it can be observed that in the case of no regularization the $rmse$ values settle to stationary levels after 6 to 8 iterations. However, the numerical results presented in Figure 3 show that whilst the retrieval of $h(t)$, see Figure 3(a), is very accurate, instabilities manifest in the unregularized solutions for the coefficients $c_1(t)$ and $c_2(t)$, see Figures 3(b) and 3(c), respectively. Note that although there is no random noise numerically simulated through (23), there still exists some small numerical noise caused by the discrepancy between the FDM direct problem numerical solution with a fixed mesh size and the exact values of the data (26). Thus the instabilities for the unregularized solution illustrated in Figures 3(b) and 3(c) show that the inverse coefficient identification problem is ill-posed in the coefficients $c_1(t)$ and $c_2(t)$. These will be even more amplified when later on we will include noise in the data (23). Including a small regularization in (21) alleviates this instability, as shown in the regularized numerical results in Figures 2 and 3. The choice of $\beta_1 = 0$, $\beta_2 = \beta_3 = 10^{-8}$ is of course not optimal and in fact these regularization parameters may still be too small, see for example, the occurrence of minima in the $rmse$ values after a certain number of iterations. But overall, corroborated with the more stable results achieved in Figures 3(b) and 3(c), it shows that regularization is required in order to obtain stable solutions for the coefficients $c_1(t)$ and $c_2(t)$. Finally, by inspecting Figures 3(a) and 4 it can be seen that the inverse problem seems stable in the components $h(t)$ and $v(y, t)$ of the solution for which regularization is not necessary. Based on this argument we shall take $\beta_1 = 0$, i.e. we do not penalise \mathbf{h} in (21) (or (22)), in the remaining of the paper.

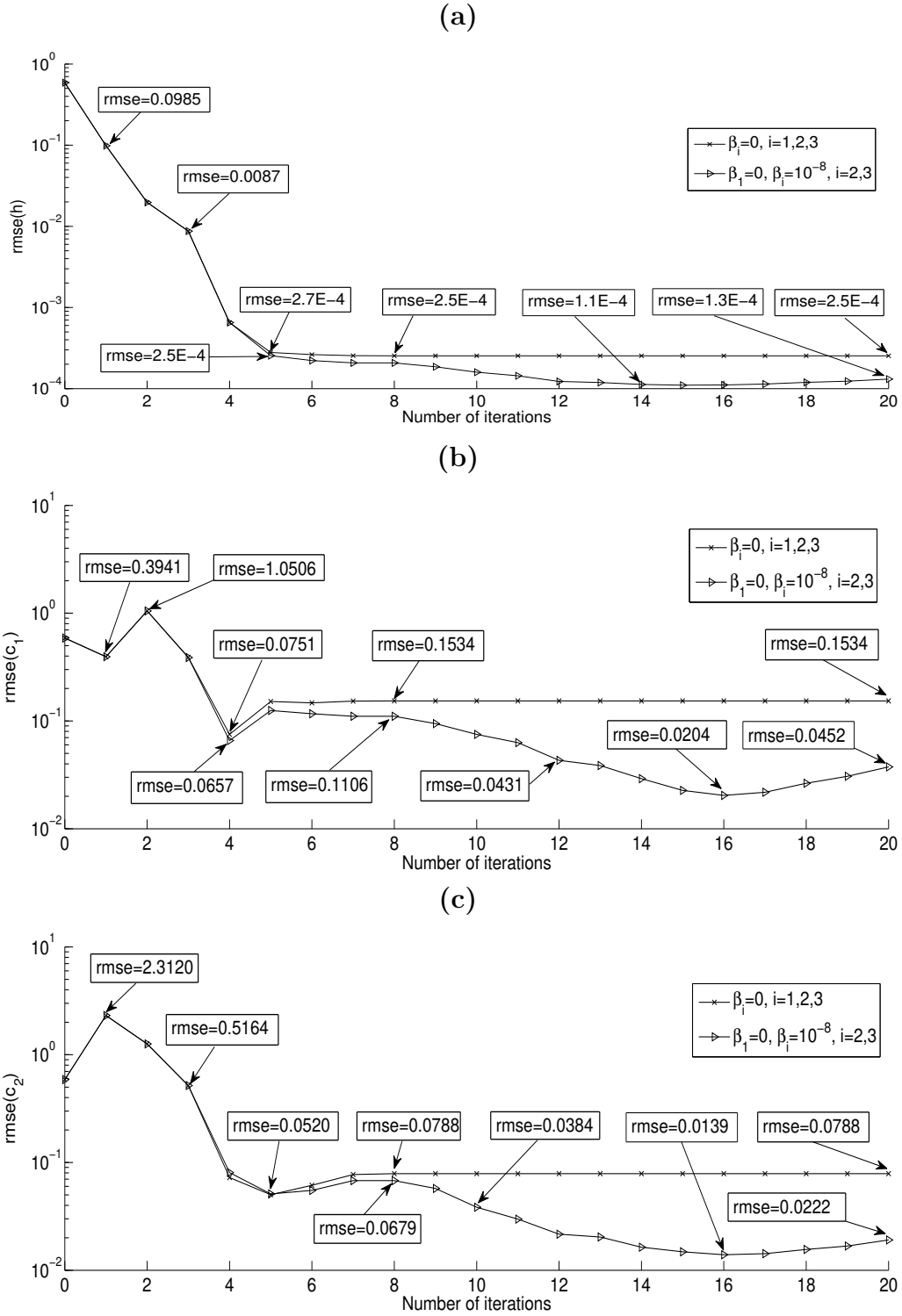


Figure 2: The $rmse$ values: (a) $rmse(h)$, (b) $rmse(c_1)$ and (c) $rmse(c_2)$, as functions of the number of iterations, no noise, with and without regularization, for Example 1.

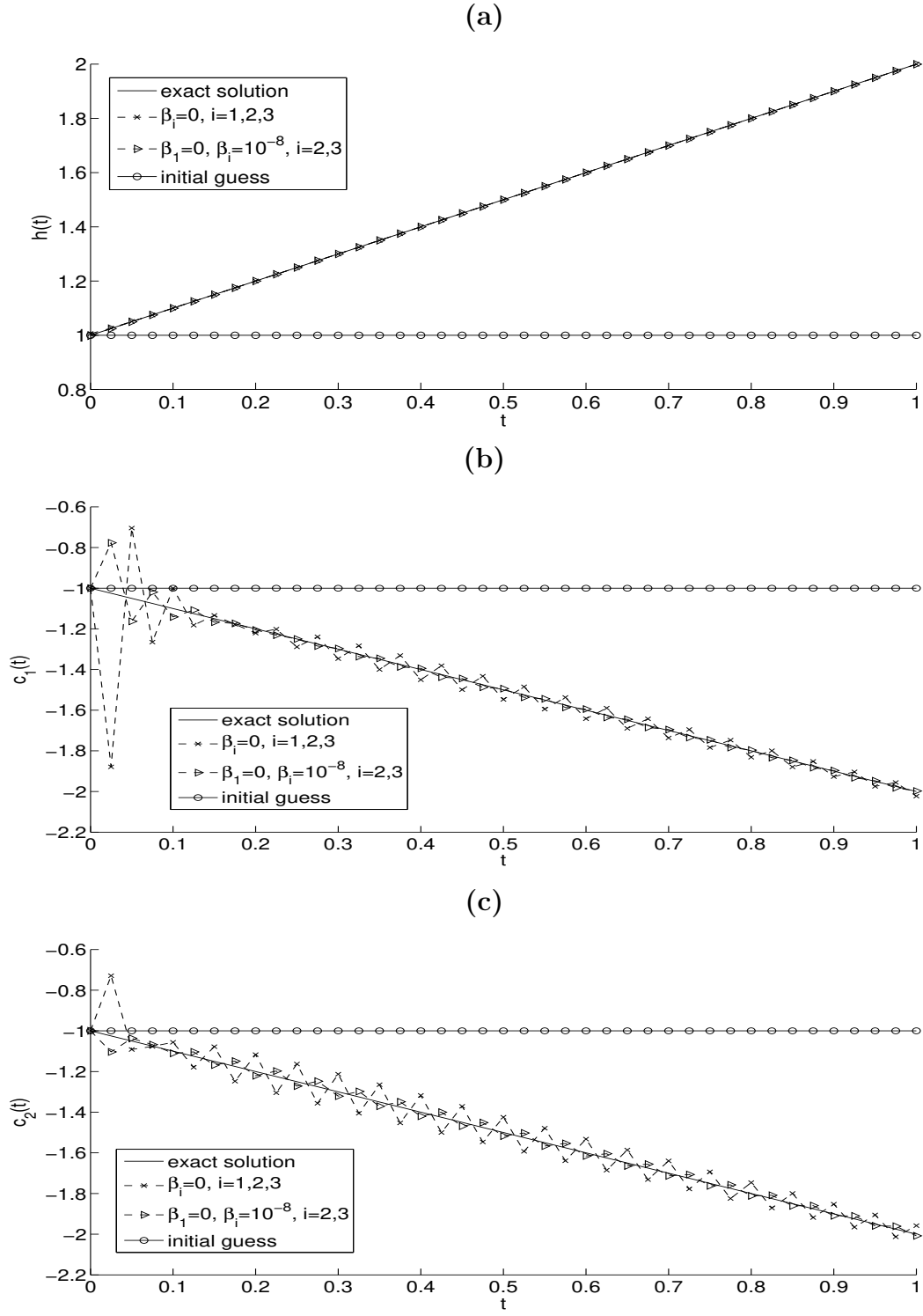


Figure 3: The exact (27) and numerical solutions for: (a) $h(t)$, (b) $c_1(t)$ and (c) $c_2(t)$, no noise, with and without regularization, for Example 1.

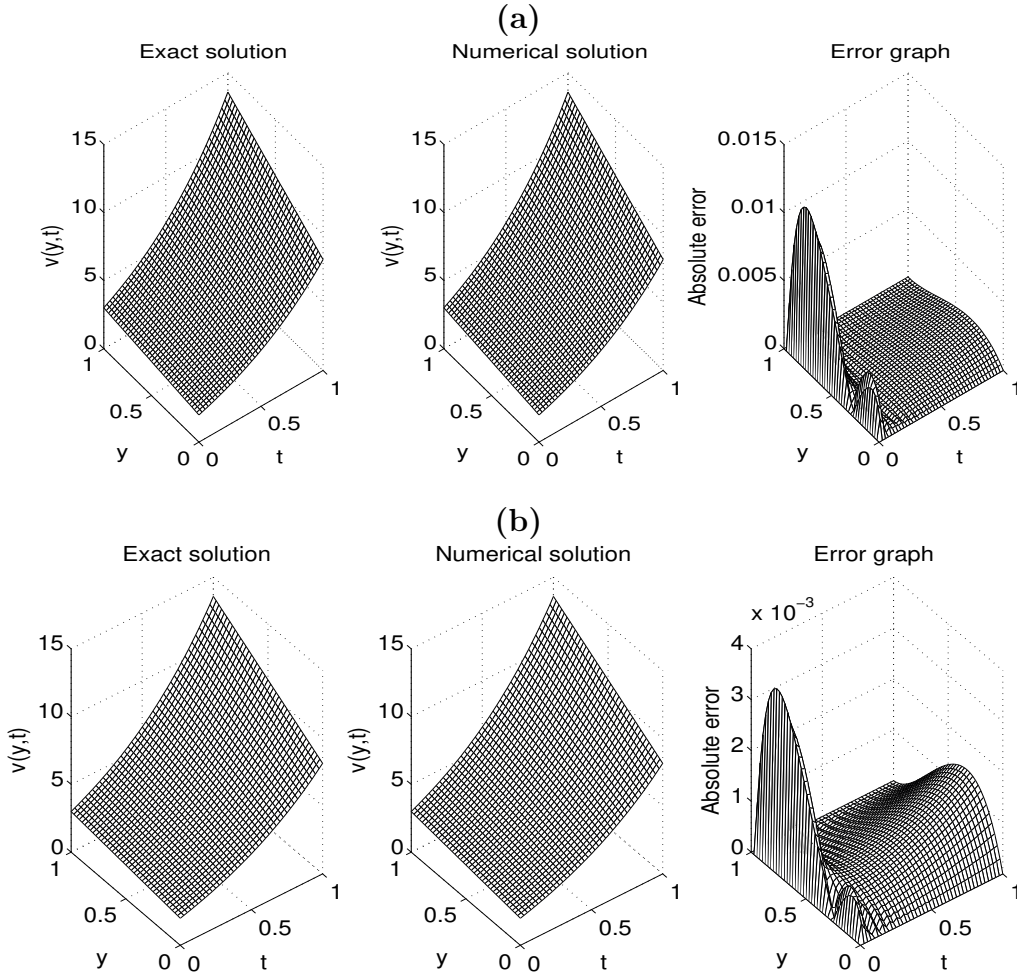


Figure 4: The exact (29) and numerical solutions for the transformed temperature $v(y, t)$, for Example 1, no noise, with (a) $\beta_i = 0, i = 1, 2, 3$ and (b) $\beta_1 = 0, \beta_i = 10^{-8}, i = 2, 3$. The absolute error between them is also included.

Next, we add a small amount of $p = 0.01\%$ noise to the data $\mu_3(t), \mu_4(t)$ and $\mu_5(t)$, as in (23), in order to model the errors which are inherently present in any practical measurement and moreover, to investigate the stability of the numerical results. We have also experimented with higher amounts of noise p in equation (24), but the results obtained were less accurate and therefore they are not presented. From the previous analysis, we anticipate that the regularization is needed in order to achieve stable and accurate results because the problem is ill-posed and very sensitive to noise. The decreasing convergence of the objective function (21), as a function of the number of iterations, is shown in Figure 5 with and without regularization. Notice that the total amount of noise included in the input data when $p = 0.01\%$ is 0.0220.

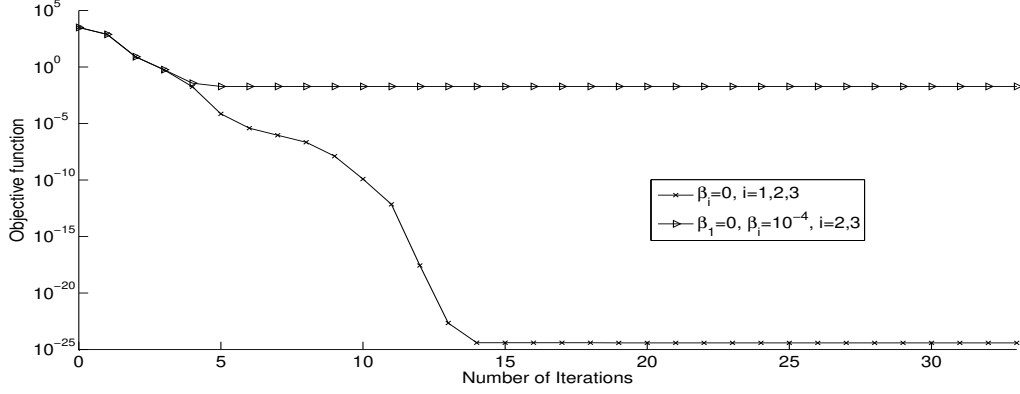


Figure 5: The objective function (21), as a function of a number of iterations, $p = 0.01\%$ noise, with and without regularization, for Example 1.

As previously argued, since there is no need to regularize the free boundary $h(t)$ we fix $\beta_1 = 0$. Also, taking $\beta_2 = \beta_3$, as positive regularization parameters in (21), the L-curve, [9], for the choice of the regularization parameter is shown in Figure 6, by plotting the solution norm $\sqrt{\|\mathbf{h}\|^2 + \|\mathbf{c}_1\|^2 + \|\mathbf{c}_2\|^2}$, as a function of the residual norm given by square root of the sum of first three terms in the right-hand side of (21). From this figure, it can be seen that regularization parameters near the "corner" of the L-curve are $\beta_2 = \beta_3 \in \{10^{-6}, 10^{-5}, 10^{-4}\}$.

The exact and numerical solutions for the free boundary $h(t)$, and the coefficients $c_1(t)$ and $c_2(t)$, with and without regularization are shown in Figure 7. From this figure, it can be noticed that the accurate and stable results are achieved for the free boundary $h(t)$ both with and without regularisation, but unstable results are obtained for the coefficients $c_1(t)$ and $c_2(t)$, if no regularization is imposed with $rmse(c_1) = 0.5645$ and $rmse(c_2) = 0.5949$. In order to stabilise the coefficients $c_1(t)$ and $c_2(t)$, we employed regularization with $\beta_1 = 0$, $\beta_2 = \beta_3 = 10^{-4}$ (given by the L-curve in Figure 6), obtaining $rmse(c_1) = 0.1089$ and $rmse(c_2) = 0.1040$. Finally, the numerical solutions for $v(y, t)$ were obtained stable and accurate and, for brevity, they are not presented.

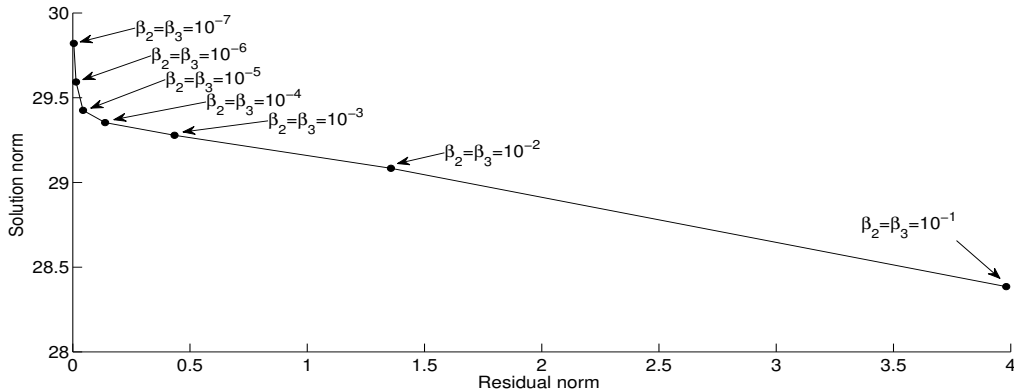


Figure 6: The residual norm versus the solution norm for various regularization parameters $\beta_2 = \beta_3 \in \{10^{-i} | i = \overline{1, 7}\}$, for Example 1 with $p = 0.01\%$ noise.

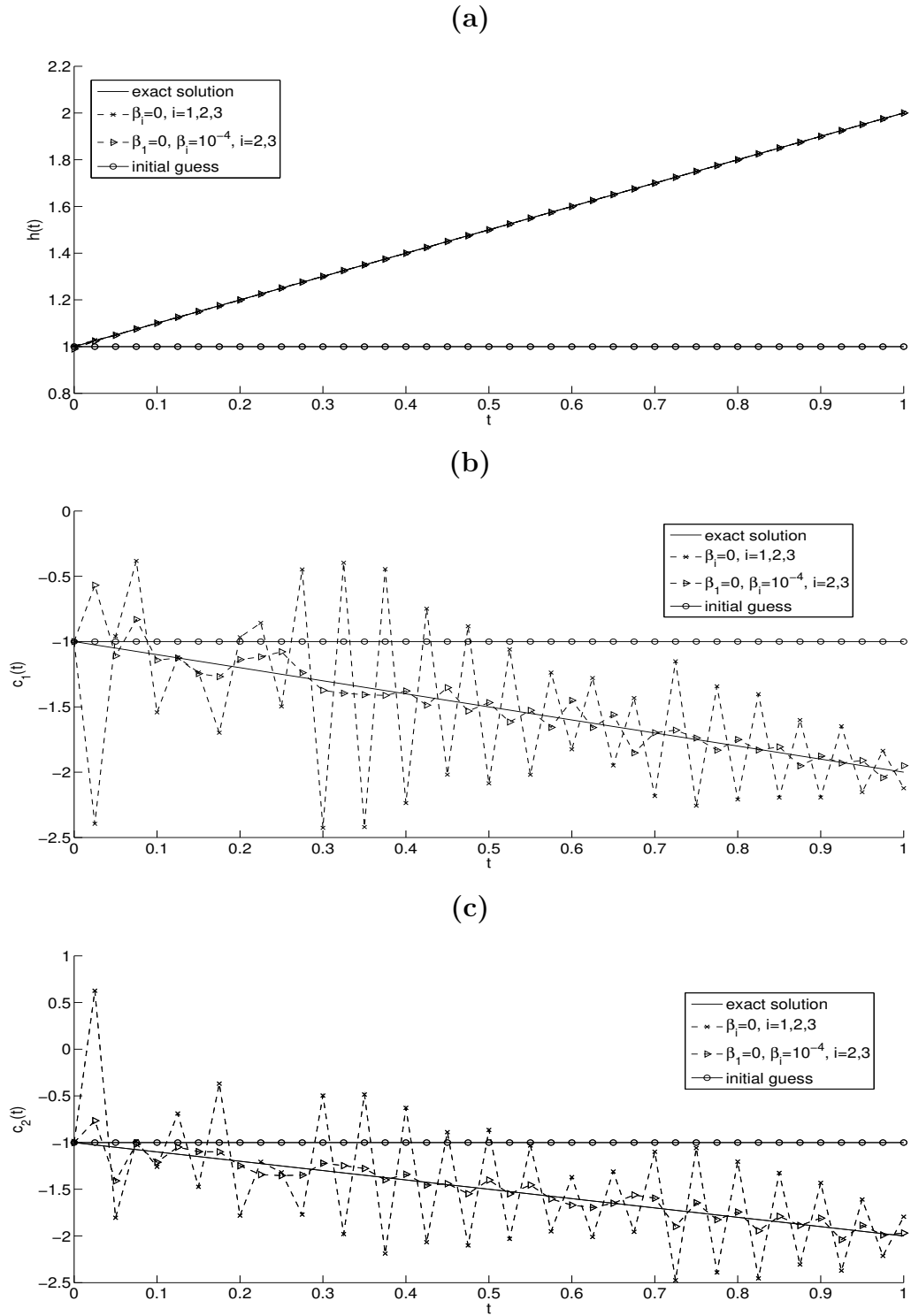


Figure 7: The exact (27) and numerical solutions for: (a) $h(t)$, (b) $c_1(t)$ and (c) $c_2(t)$, $p = 0.01\%$ noise, with and without regularization, for Example 1.

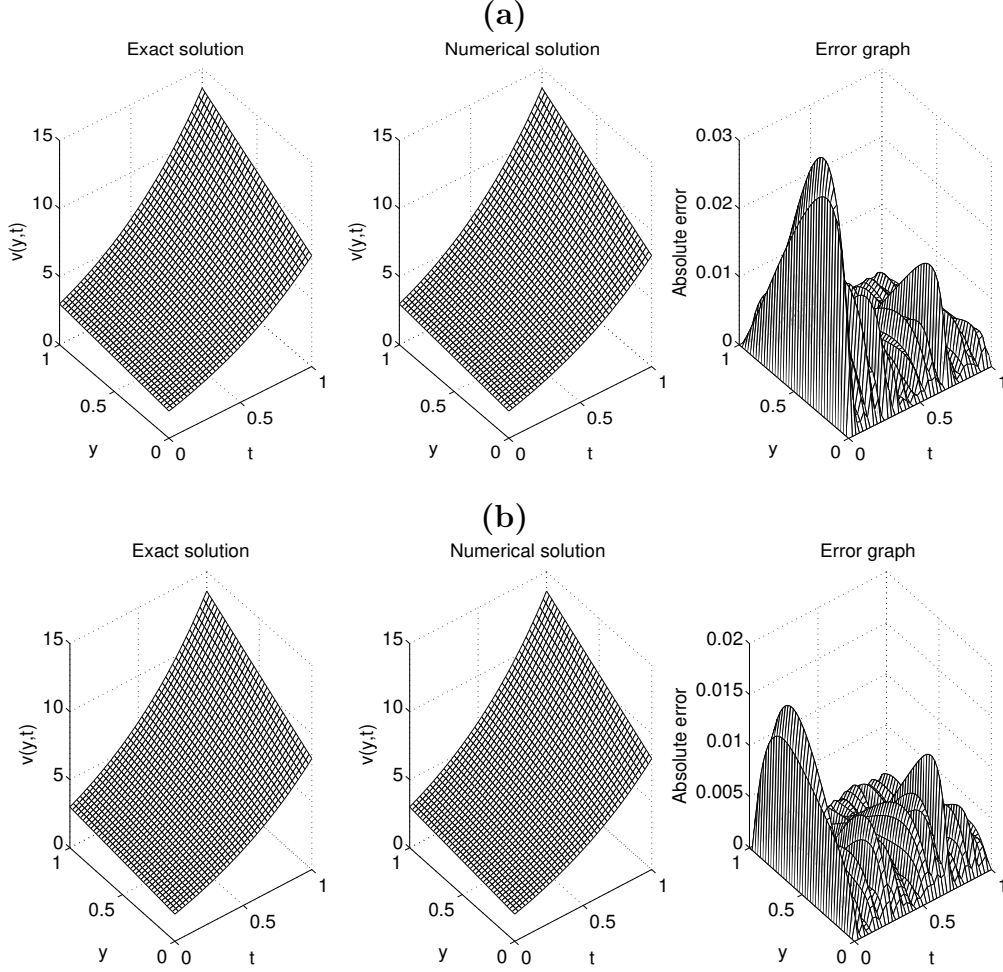


Figure 8: The exact (29) and numerical solutions for the transformed temperature $v(y, t)$, for Example 1, $p = 0.01\%$ noise, with (a) $\beta_i = 0, i = 1, 2, 3$ and (b) $\beta_1 = 0, \beta_i = 10^{-4}, i = 2, 3$. The absolute error between them is also included.

5.2 Example 2

In this example we consider the second inverse problem given by equations (1)–(3), (5), (6) and (17), with the same input data (26) as in Example 1, except that the data $\mu_3(t)$ given by equation (4) is replaced by the second-order heat moment $\mu_6(t)$ given by equation (18) as

$$\mu_6(t) = \frac{1}{12}e^t(t+1)^3(7t+11), \quad t \in [0, 1]. \quad (31)$$

Also, the initial guesses for the vectors \mathbf{h} , \mathbf{c}_1 and \mathbf{c}_2 are given by equation (30), the same as in Example 1.

Figures 9–16 for Example 2 are the corresponding analogue of Figures 1–8 for Example 1 and, in order to avoid repetition, we shall discuss below only the main similarities and differences between the two examples.

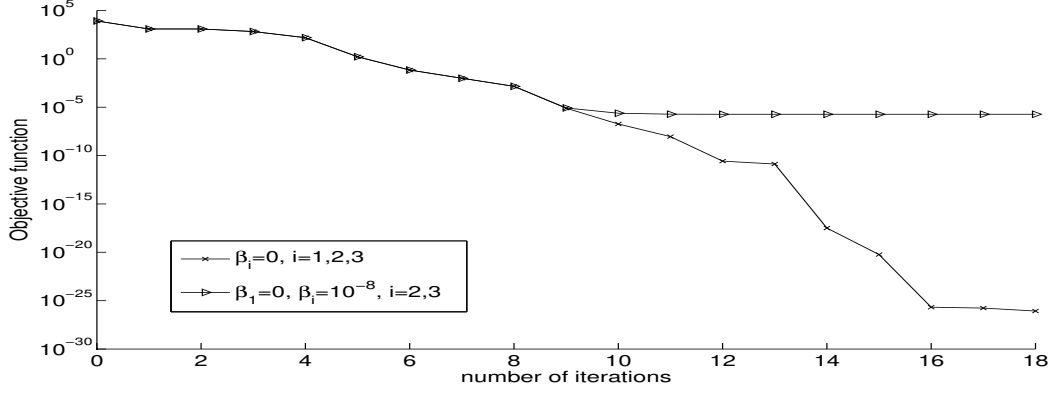


Figure 9: The objective function (22), as a function of a number of iterations, no noise, with and without regularization, for Example 2.

Whilst all the results of Examples 1 and 2 are consistent in terms of the numerical regularization method employed being accurate and stable, overall one can see that the second inverse problem (Example 2) is more ill-posed than the first inverse problem (Example 1). This can be seen by:

- (i) the larger number of iterations required to achieve convergence in the case of no noise (compare Figures 1 and 9);
- (ii) the more enhanced non-monotonic behaviour of the *rmse* curves (compare Figures 2 and 10);
- (iii) the higher and larger oscillations manifested in retrieving the coefficients $c_1(t)$ and $c_2(t)$ in case of no regularization (compare Figures 3, 7 and 11, 15);
- (iv) the larger *rmse* values, as illustrated by the comparison shown in Table 1.

Table 1: The *rmse* values for Examples 1 and 2.

Example 1	$rmse(h)$	$rmse(c_1)$	$rmse(c_2)$
$p = 0, \beta_1 = \beta_2 = 0$	2.5E-4	0.1534	0.0788
$p = 0, \beta_1 = \beta_2 = 10^{-8}$	1.3E-4	0.0452	0.0222
$p = 0.01\%, \beta_1 = \beta_2 = 0$	6.1E-4	0.5645	0.5949
$p = 0.01\%, \beta_1 = \beta_2 = 10^{-4}$	4.7E-4	0.1089	0.1040
Example 2	$rmse(h)$	$rmse(c_1)$	$rmse(c_2)$
$p = 0, \beta_1 = \beta_2 = 0$	6.8E-4	0.4892	0.4480
$p = 0, \beta_1 = \beta_2 = 10^{-8}$	6.8E-4	0.1968	0.0504
$p = 0.01\%, \beta_1 = \beta_2 = 0$	3.3E-3	6.6965	3.7308
$p = 0.01\%, \beta_1 = \beta_2 = 10^{-4}$	2.2E-3	0.3587	0.2376

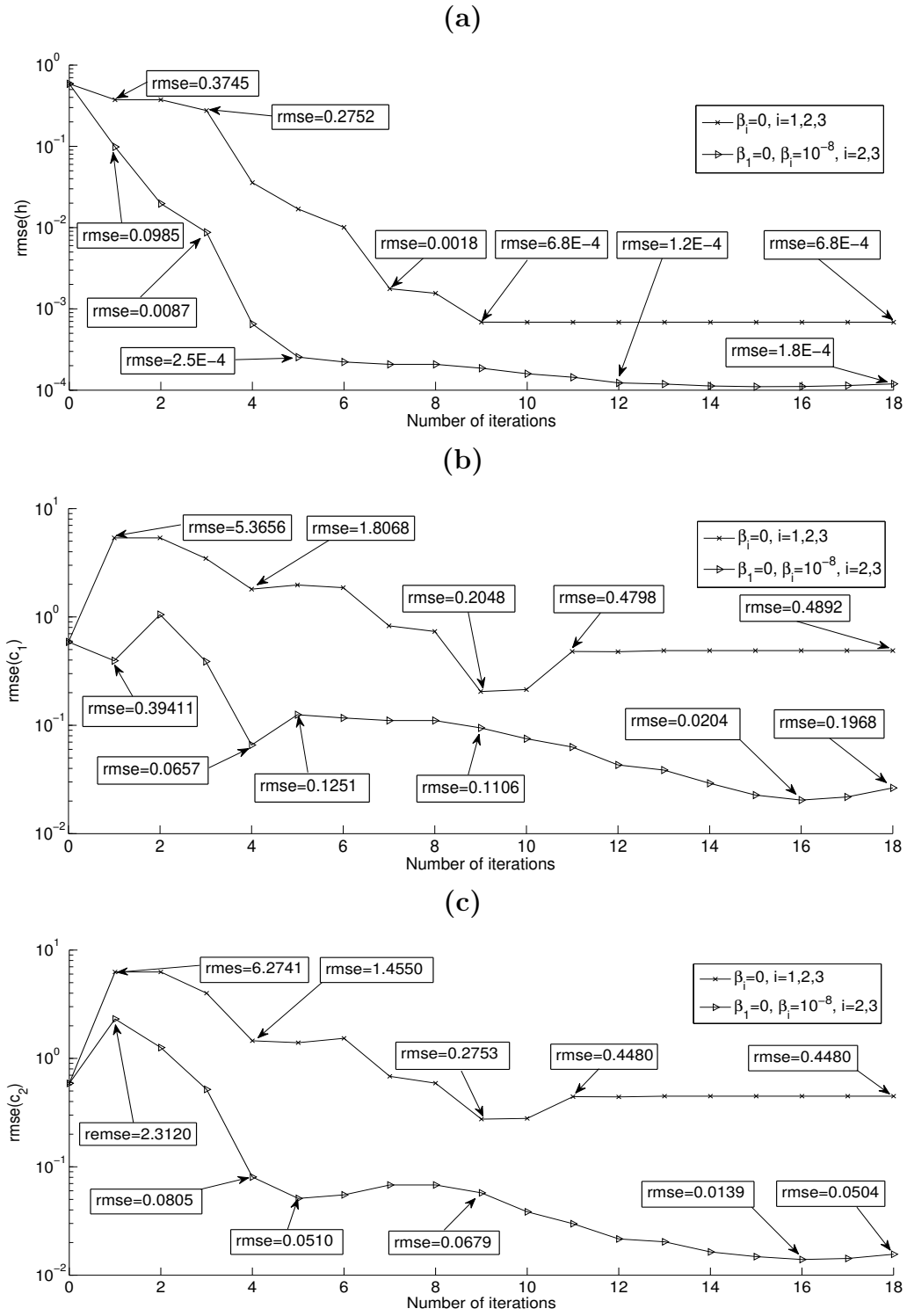


Figure 10: The $rmse$ values: (a) $rmse(h)$, (b) $rmse(c_1)$ and (c) $rmse(c_2)$, as functions of the number of iterations, no noise, with and without regularization, for Example 2.

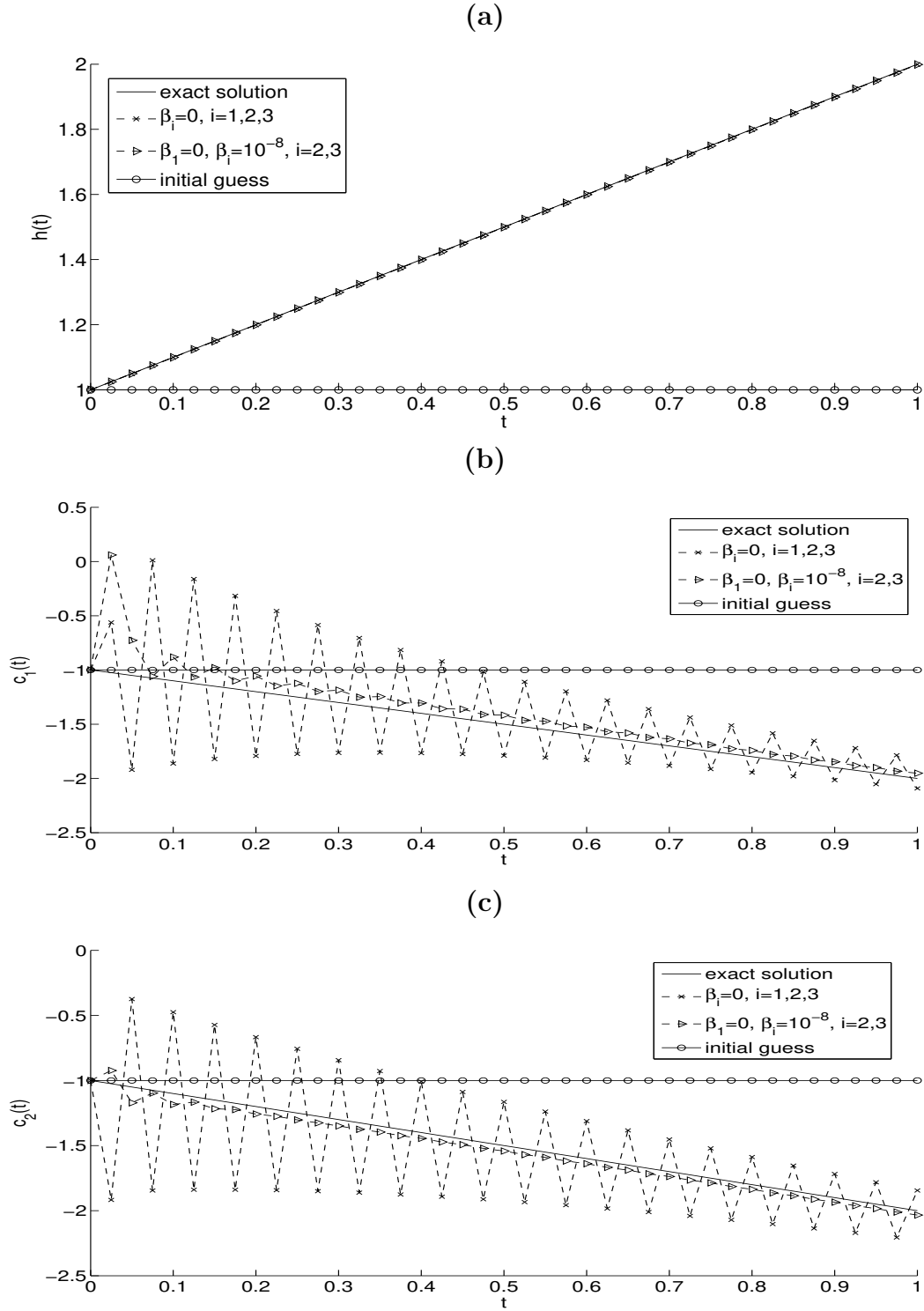


Figure 11: The exact (27) and numerical solutions for: (a) $h(t)$, (b) $c_1(t)$ and (c) $c_2(t)$, no noise, with and without regularization, for Example 2.

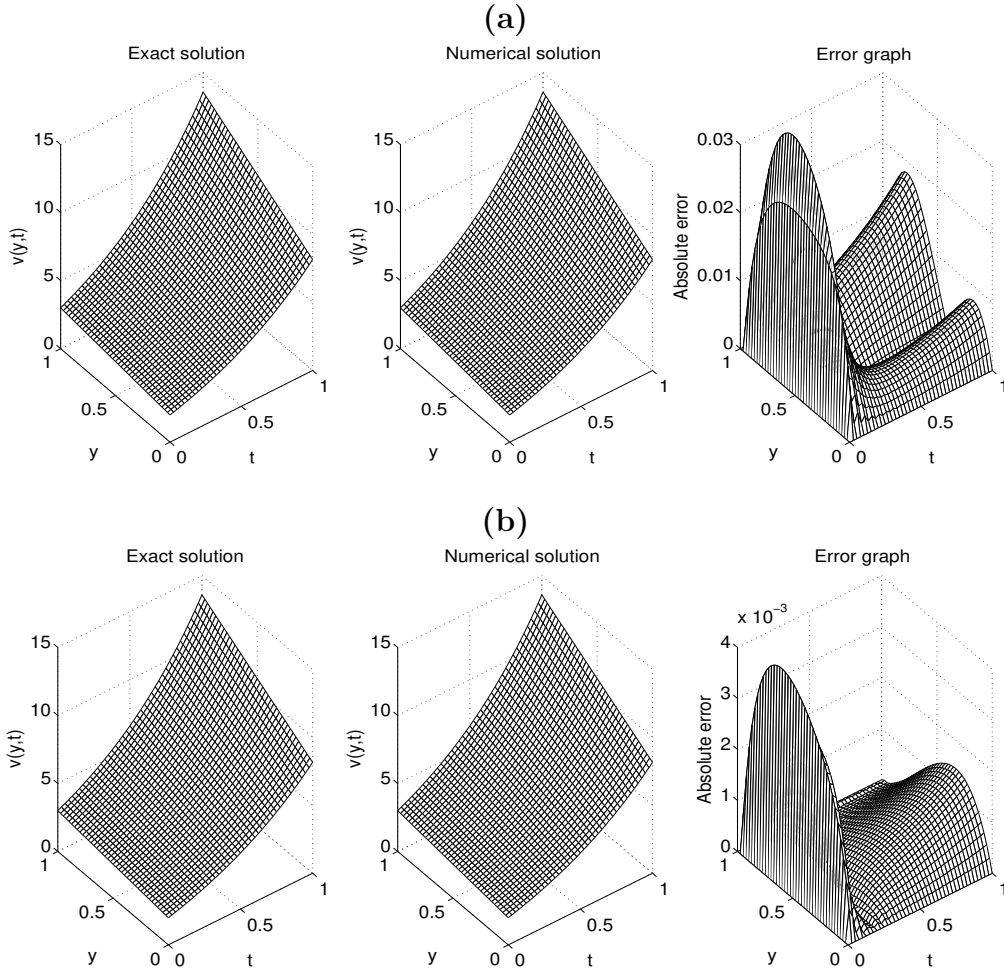


Figure 12: The exact (29) and numerical solutions for the transformed temperature $v(y,t)$, for Example 2, no noise, with (a) $\beta_i = 0, i = 1, 2, 3$ and (b) $\beta_1 = 0, \beta_i = 10^{-8}, i = 2, 3$. The absolute error between them is also included.

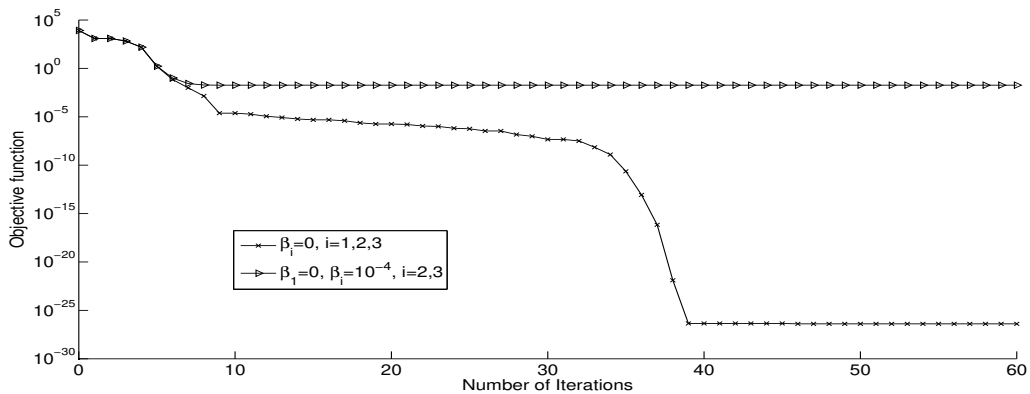


Figure 13: The objective function (22), as a function of a number of iterations, $p = 0.01\%$ noise, with and without regularization, for Example 2. Notice that the total amount of noise included in the input data when $p = 0.01\%$ is 0.0349.

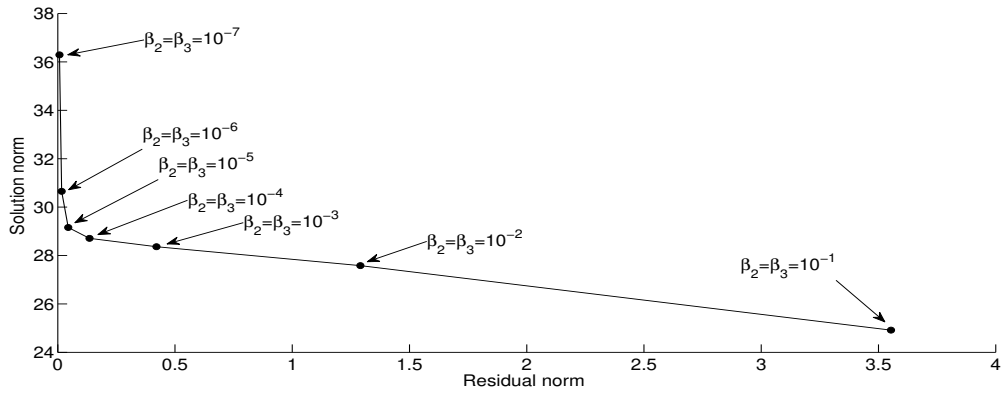


Figure 14: The residual norm (given by the square root of the first three terms in the right-hand side of (22)) versus the solution norm for various regularization parameters $\beta_2 = \beta_3 \in \{10^{-i} | i = \overline{1, 7}\}$, for Example 2 with $p = 0.01\%$ noise.

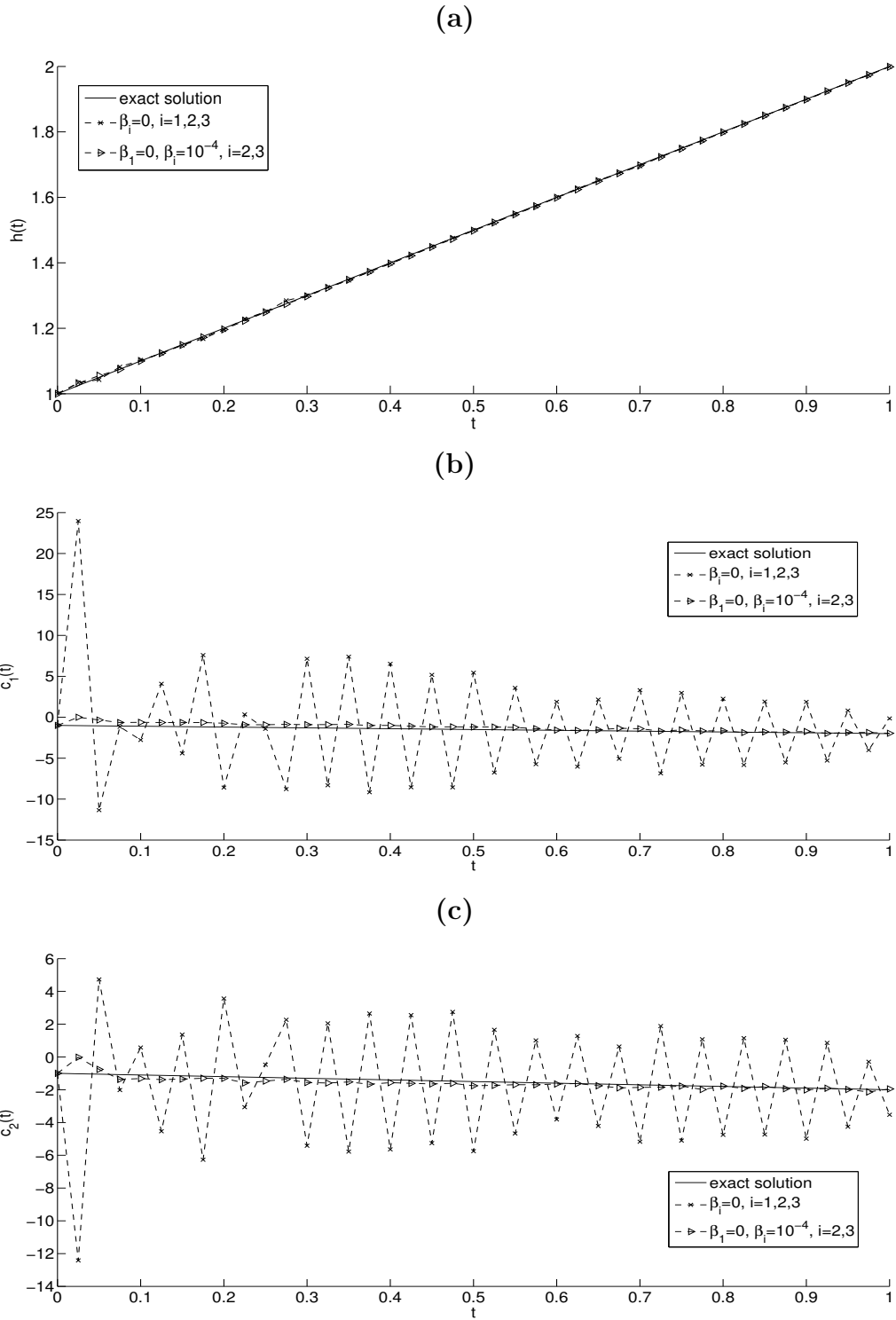


Figure 15: The exact (27) and numerical solutions for: (a) $h(t)$, (b) $c_1(t)$ and (c) $c_2(t)$, $p = 0.01\%$ noise, with and without regularization, for Example 2.

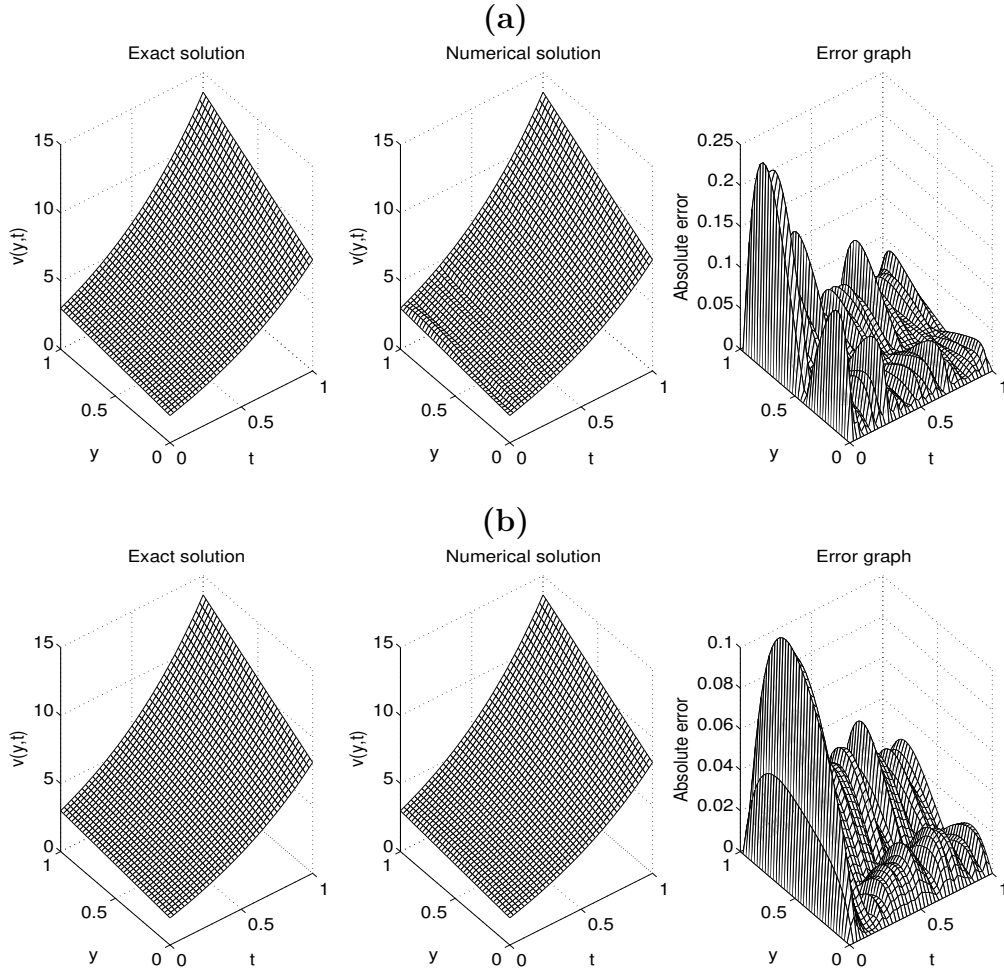


Figure 16: The exact and numerical solutions for the transformed temperature $v(y,t)$, for Example 2, $p = 0.01\%$ noise, with (a) $\beta_i = 0, i = 1, 2, 3$ and (b) $\beta_1 = 0, \beta_i = 10^{-4}, i = 2, 3$. The absolute error between them is also included.

6 Conclusions

In this paper, inverse nonlinear problems consisting of simultaneously identifying time-dependent reaction coefficients in the heat equation with a free boundary have been investigated. The direct solver based on the FDM with the Crank-Nicolson scheme has been employed. The inverse problem was solved using the MATLAB optimisation toolbox routine *lsqnonlin* for minimizing the nonlinear Tikhonov regularization functional. The accuracy and stability of the numerical results for the two inverse problems, for Examples 1 and 2, have been assessed. Based on the numerical results and discussion we can conclude that the Stefan condition (4) contains more information than the second-order heat moment condition (17). Although not illustrated, it is reported that similar conclusions have been obtained for many other numerical tests that we have investigated including the recovery of non-smooth reaction coefficients. Extension to the case when both sides of the finite slab are free boundaries, [20, 22], will be the subject of future work.

Acknowledgments

M.J. Huntul would like to thank Jazan University in Saudi Arabia and United Kingdom Saudi Arabian Cultural Bureau (UKSACB) in London for supporting his PhD at the University of Leeds. Discussions with Dr M.S. Hussein are acknowledged.

References

- [1] Beilina, L. and Klibanov, M.V. (2012) *Approximate Global Convergence and Adaptivity of Coefficient Inverse Problems*, Springer, New York.
- [2] Broadbridge, P., Tritscher, P. and Avagliano, A. (1993) Free boundary problems with nonlinear diffusion, *Mathematical and Computer Modelling*, **18**, 15–34.
- [3] Borukhov, V.T. and Kostyukova, O.I. (2013) Identification of time-dependent coefficients of heat transfer by the methods of suboptimal stage-by-stage optimization, *International Journal of Heat and Mass Transfer*, **59**, 286–294.
- [4] Coleman, T.F. and Li, Y. (1996) An interior trust region approach for nonlinear minimization subject to bounds, *SIAM Journal on Optimization*, **6**, 418–445.
- [5] Crank, J. (1984) *Free and Moving Boundary Problems*, Clarendon Press, Oxford.
- [6] Engl, H.W., Hanke, M. and Neubauer, A. (2000) *Regularization of Inverse Problems*, Kluwer Academic Publishers, Dordrecht.
- [7] Goldman, N.L. (1997) *Inverse Stefan Problems*, Springer Science & Business Media, Berlin.
- [8] Huntul, M.J., Lesnic, D. and Hussein, M.S. (2017) Reconstruction of time-dependent coefficients from heat moments, *Applied Mathematics and Computation*, **301**, 233–253.
- [9] Hansen, P.C. (1992) Analysis of discrete ill-posed problems by means of the L-curve. *SIAM Review*, **34**, 561–580.
- [10] Hussein, M.S., Lesnic, D., Ivanchoy, M.I. and Snitko, H.A. (2016) Multiple time-dependent identification thermal problems with a free boundary, *Applied Numerical Mathematics*, **99**, 42–50.
- [11] Hussein, M.S. and Lesnic, D. (2014) Determination of a time-dependent thermal diffusivity and free boundary in heat conduction, *International Communications in Heat and Mass Transfer*, **53**, 154–163.
- [12] Hussein, M.S., Lesnic, D. and Ivanchoy, M. (2013) Free boundary determination in nonlinear diffusion, *East Asian Journal on Applied Mathematics*, **3**, 295–310.
- [13] Hon, Y.C. and Li, M. (2008) A computational method for inverse free boundary determination problem, *International Journal for Numerical Methods in Engineering*, **73** (9):1291-1309.

- [14] Johansson, B.T., Lesnic, D. and Reeve, T. (2011) A method of fundamental solutions for the one-dimensional inverse Stefan problem, *Applied Mathematical Modelling*, **35**(9):4367-4378.
- [15] Lesnic, D., Yousefi, S.A. and Ivanchov, M. (2013) Determination of a time-dependent diffusivity from nonlocal conditions, *Journal of Applied Mathematics and Computing*, **41**(1-2):301-320.
- [16] Mathworks (2012) Documentation Optimization Toolbox-Least Squares (Model Fitting) Algorithms, available at www.mathworks.com.
- [17] Malyshev, I.G. (1975) Inverse problems for the heat-conduction equation in a domain with a moving boundary, *Ukrainian Mathematical Journal*, **27**, 568–572.
- [18] Snitko, H.A. (2010) Coefficient inverse problem for a parabolic equation in a domain with free boundary, *Journal of Mathematical Science*, **167**, 30–46.
- [19] Snitko, H.A. (2012) Inverse problem for determination of time-dependent coefficients of a parabolic equation in a free-boundary domain, *Journal of Mathematical Science*, **181**, 350–365.
- [20] Snitko, H.A. (2014) On a coefficient inverse problem for a parabolic equation in a domain with free boundary, *Journal of Mathematical Sciences*, **200**, 374–388.
- [21] Snitko, H.A. (2014) Inverse problem of finding time-dependent functions in the minor coefficient of a parabolic equation in the domain with free boundary, *Journal of Mathematical Science*, **203**, 40–54.
- [22] Snitko, H.A. (2014) Determination of the lowest coefficient for a one-dimensional parabolic equation in a domain with free boundary, *Ukrainian Mathematical Journal*, **65**, 1698–1719.
- [23] Trucu, D., Ingham, D.B. and Lesnic, D. (2011) Reconstruction of the space- and time-dependent blood perfusion coefficient in bio-heat transfer, *Heat Transfer Engineering*, **32**, 800–810.